

Electronic Properties of Au Nano-Particles Supported on Stoichiometric and Reduced TiO₂(110) Substrates

T. Okazawa¹, M. Kohyama¹ and Y. Kido²

Abstract

Growth modes and electronic properties were analyzed for Au nano-particles grown on stoichiometric and reduced TiO₂(110) substrates by medium energy ion scattering (MEIS) and photoelectron spectroscopy (PES) using synchrotron-radiation-light. Initially, two-dimensional islands (2D) with a height of one and two atomic layers grow and higher coverage increases the islands height to form three-dimensional (3D) islands for the stoichiometric TiO₂(110) substrate. In contrast, 3D islands start to grow from initial stage with a small Au coverage (≥ 0.1 ML, 1 ML = 1.39×10^{15} atoms/cm²: Au(111)) probably due to O-vacancies acting as a nucleation site. Above 0.7 ML, all the islands become 3D ones taking a shape of a partial sphere and the Au-clusters change to metal for both substrates. We observed the Au 4f and Ti 3p core level shifts together with the valence band spectra. The Ti 3p peak for the O-deficient surface shifts to higher binding energy by 0.25 ± 0.05 eV compared to that for the stoichiometric surface, indicating downward band bending by an electron charge transfer from an O-vacancy induced surface-state band to n-type TiO₂ substrate. Higher binding energy shifts of Au 4f peaks observed for both substrates reveal an electron charge transfer from Au to TiO₂ substrates. The work functions of Au nano-particles supported on the stoichiometric and reduced TiO₂ substrates were also determined as a function of Au coverage and explained clearly by the above surface and interface dipoles.

¹ National Institute of Advanced Industrial Science and Technology, AIST Kansai,
Midorigaoka 1-8-31, Ikeda, Osaka 563-8577, Japan

² Department of Physics, Ritsumeikan University, Kusatsu, Shiga-ken 525-8577, Japan

1. Introduction

It has been recognized that Au is the most noble of all metals until an epoch finding pronounced catalytic activities of Au-nano-particles supported on transition-metal oxides[1,2]. Hammer and Nørskov[3] showed, for an example of H₂ dissociation on metal surfaces that the H 1s – d(metal) anti-bonding states are filled for Au and the coupling matrix element V_{sd} takes a large value because of the expanding 5d orbitals of Au thus resulting in formation of a large energy barrier for H₂ dissociation. Here, we must note that the above discussion is applied to bulk crystals but not to nano-size particles. Haruta [1,2] first found high catalytic activities of nano-size Au clusters deposited on oxide supports, such as TiO₂, Fe₂O₃, Co₃O₄ and NiO for CO oxidation. Since that, many investigations not only experiments and also theoretical calculations have been reported, in particular for Au nano-particles on TiO₂[4-10]. Almost of all works are concentrated on the size effect upon catalytic activity. Lopez and Nørskov[11] claimed that the catalytic activity depends on the cluster structure rather than metal-support interaction. Recently, however, it was pointed out that an electron charge transfer plays an important role to highly activate adsorbed O₂ molecules[12-13]. Several studies on the electronic properties of Au nano-particles supported on TiO₂ have been performed mainly by scanning tunneling microscope and spectroscopy (STM/STS) for very low coverage of Au[9, 14-18].

In the previous work[19], we clarified the growth mode and electronic structure of Au nano-particles grown on NiO(001) and stoichiometric TiO₂(110). Some recent papers reported that a pronounced electron charge transfer takes place between Au and reduced TiO₂ and it plays a significant role to enhance CO oxidation[9,20-22]. In this study, we prepared stoichiometric (S) and reduced (R) TiO₂(110) surfaces and analyzed quantitatively the growth mode and electronic properties of Au nano-particles deposited on the above substrates for Au-coverage from 0.1 up to 8.5 ML (1 ML = 1.39×10^{15} atoms/cm²: corresponding to the areal density of Au(111)) by high-resolution medium energy ion scattering (MEIS)[23,24] and photoelectron spectroscopy (PES) using synchrotron-radiation(SR)-light. The absolute amount of O-vacancies was estimated using isotopically labeled ¹⁸O₂. We determined the

work functions of Au nano-particles supported on the TiO₂ surfaces by the photo-emission spectra from samples biased negatively and manifested the correlation between the electronic charge transfer and the work functions.

2. Experiment

The experiment was carried out at Beam-Line 8 named SORIS constructed at Ritsumeikan SR Center. This beam-line consists of three modules of high-resolution MEIS, SR-PES and sample preparation including molecular beam epitaxy and reflection high-energy electron diffraction (RHEED). Rutile TiO₂(110) substrates whose surfaces were mirror-polished were introduced in an ultra-high vacuum (UHV) chamber and then annealed at 800°C for 60 min to form O-vacancies. Thereby the color of the sample changed into dark blue from light yellow and the electronic property also changed into an n-type semiconductor (band gap: 3.0 eV)[25]. Sputtering by 0.75 keV Ar⁺ beams followed by annealing at 550°C for 5 min at O₂-pressure of 1×10⁻⁶ Torr led to a clean stoichiometric (1×1) surface, which was confirmed by RHEED and PES observation of the valence band spectra. Slightly reduced surfaces were obtained by annealing the above stoichiometric surface at 550-700°C for 5 min in UHV. In this case, a small peak about 0.9 eV below the Fermi level appeared in the valence band spectra, which comes from the 3d electrons of Ti adjacent an O-vacancy site[26]. The absolute amount of the O-vacancies located at the top-layer is estimated to be ~ 0.04×10¹⁵ atoms/cm² from the MEIS analysis presented below, corresponding to about 8 % of the bridging O atoms [25,27] on top for the sample annealed at 550°C for 5 min in UHV. This is quite consistent with that measured by low energy ion scattering[28]. Figure 1 shows the MEIS spectrum observed for 80 keV He⁺ incidence on the sample exposed to ¹⁸O₂ ambient at room temperature (RT) for 100 s at a pressure of 1×10⁻⁵ Torr. Indeed, the surface state band induced by O-vacancies in the top-layer disappeared for this sample (see Fig. 6, right side). Au deposition was performed at RT on the clean surface using a Knudsen cell at a rate of 0.25 - 0.35 ML/min.

The absolute amount of Au deposited was determined by MEIS using 120 keV He⁺ ions

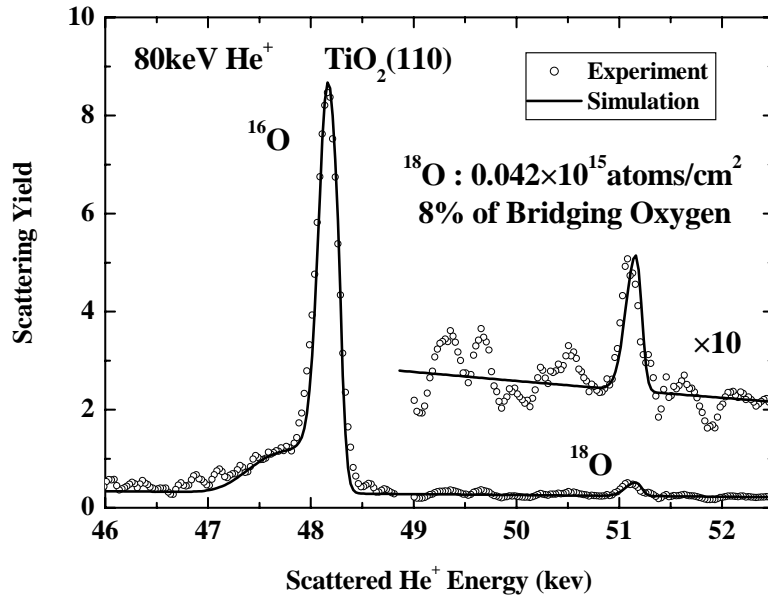


FIG.1. MEIS spectrum observed for 80 keV He^+ ions incident along the $[0\bar{1}0]$ -axis and backscattered from oxygen atoms to the $[100]$ direction of reduced $\text{TiO}_2(110)$ which was exposed to $^{18}\text{O}_2$ for 100 s at a pressure of 1×10^{-5} Torr at RT. The best-fit is obtained assuming an absolute amount of $0.042 \pm 0.005 \times 10^{15}$ $^{18}\text{O}/\text{cm}^2$ on top.

with an accuracy better than 0.005 ML. Its excellent energy resolution of 9×10^{-4} allows a layer-by-layer analysis[24] and makes it possible to derive the quantitative information on the shape and size together with the areal occupation ratio of Au islands[19]. In order to avoid any effects changing the surface structure, we shifted an ion-irradiation area after an integrated beam current of $1 \mu\text{C}$. In fact, the MEIS spectra did not change significantly after He^+ -irradiation of $\sim 5 \mu\text{C}$. The growth mode and crystallinity of the deposited Au were monitored by RHEED. Quite complementally photoelectron spectroscopy provides the information about the electronic structure of Au nano-particles supported on S- and R- $\text{TiO}_2(110)$ surfaces. In the present study, we observed the core level spectra of Au 4f and Ti 3p together with the valence band spectra using SR-light. The SR photons were monochromated by two kinds of gratings in the energy range from 10 up to 500 eV. The monochromated photon flux is maximal around 100 - 150 eV and decreases abruptly with increasing photon energy. A hemispherical electrostatic analyzer with a curvature of 139.7

mm gives an excellent energy resolution of ± 0.05 eV. The escape depths of photoelectrons observed are estimated to be less than 1 nm. The work functions of the $\text{TiO}_2(110)$ surfaces before and after Au deposition were also determined by the photoemission spectra from the samples negatively biased[19]. Incident photon energies were calibrated precisely using the 2nd and 3rd harmonic waves. All the above analyses were performed *in situ* under UHV condition ($\leq 2 \times 10^{-10}$ Torr).

3. Results and Discussion

Figure 2 shows the MEIS spectra observed for He^+ ions backscattered from Au particles supported on the S-(left side) and R- $\text{TiO}_2(110)$ for Au coverage from 0.1 to 0.7 ML. The spectra were best-fitted by inputting appropriate fitting parameters, (i) average areal occupation ratios of two-dimensional (2D) and three-dimensional (3D) islands, (ii) average height of 2D islands and (iii) diameter d and height h of 3D-islands. Here, we define the 2D-islands as the ones taking a shape of thin disks with a height below two atomic layers (2 ALs: 0.71 nm) and assumed that 3D-islands take a shape of partial sphere. In the present spectrum simulations, the geometrical edge factor was taken into account. The detail of the basic treatment how to synthesize ion scattering spectra was described elsewhere[29]. In order to make the simulations easier, the scattering geometry was fixed to the $[1\bar{1}0]$ -incidence and $[100]$ -emergence (incident angle: 45° , emergent angle: 45°). The above fitting parameters giving the best-fit are indicated in Figs. 3 and 4. In the case of S- $\text{TiO}_2(110)$, initially 2D-islands grow dominantly for Au coverage up to 0.5 ML and further agglomeration with higher coverage leads to growth of 3D-islands. In contrast, 2D-island growth is limited within a very early stage (≤ 0.2 ML) and 3D-islands start to grow from an initial stage for the R- $\text{TiO}_2(110)$. This is probably due to O-vacancies acting as a nucleation site. However, for Au coverage above 1 ML, all the islands become three-dimensional and take a shape of partial sphere with almost a same size for the S- and R- TiO_2 supports. The height and diameter of the partial sphere increase linearly with increasing Au coverage from 1 ML up to 8.5 ML (not shown here).

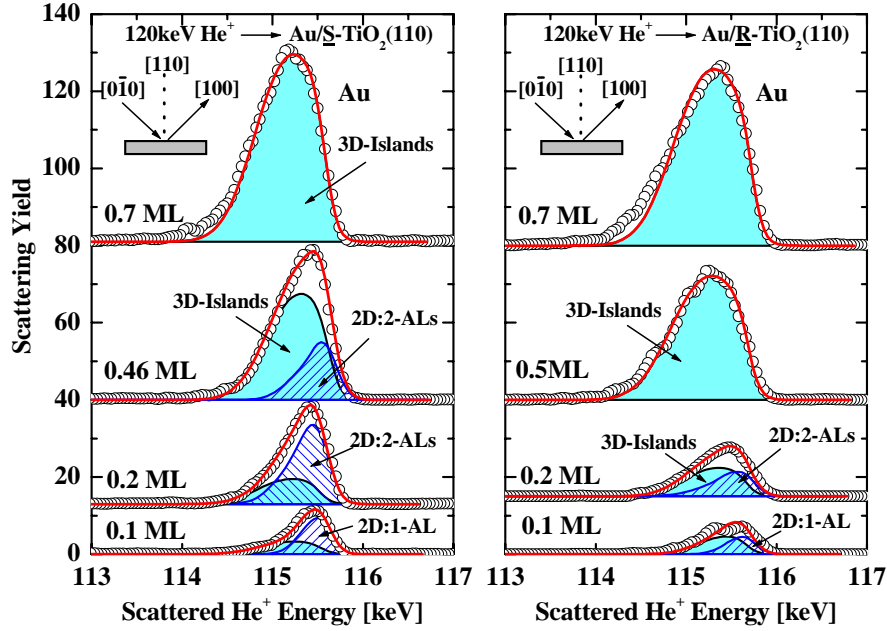


FIG.2. Observed MEIS spectra (open circles) for 120 keV He^+ ions incident along $[0\bar{1}0]$ -axis and backscattered to $[100]$ direction as a function of Au coverage supported on stoichiometric (left) and reduced (right) $\text{TiO}_2(110)$ substrates. Best-fitted spectra are obtained assuming appropriate fitting parameters indicating in Figs. 3 and 4, (i) occupation ratios of 2D and 3D islands, (ii) average diameter and height of a partial sphere of Au 3D-islands and (iii) height of 2D islands. Here, 1-AL and 2-ALs mean one and two atomic-layer height, respectively.

We observed the valence band spectra at photon energy of 49.6 eV as a function of Au coverage, which are shown in Fig. 5(a) (R- TiO_2). Except for the surface state band, the spectra for Au/R- TiO_2 are basically similar to those for Au/S- TiO_2 . Magnified spectra near the Fermi edge are shown in Figs. 5(b) and (c) for R- TiO_2 and S- TiO_2 substrates, respectively. The growing broad peaks below the Fermi level for the Au/S- TiO_2 originate from the Au 6s band. In the case of Au/R- TiO_2 , if one considers the contribution from the growing Au 6s band, it is seen that the intensity of the broad peak induced by the O-vacancies in the bridging O rows is decreased by Au deposition. This also indicates the O-vacancy acting as a nucleation site for Au nano-clusters. Such a behavior was directly observed by Wahlström et al.[17] using STM/STS. The pronounced peaks seen just below the Fermi level for both substrates at Au coverage of 8.5 ML correspond to the Shockley surface state generated on

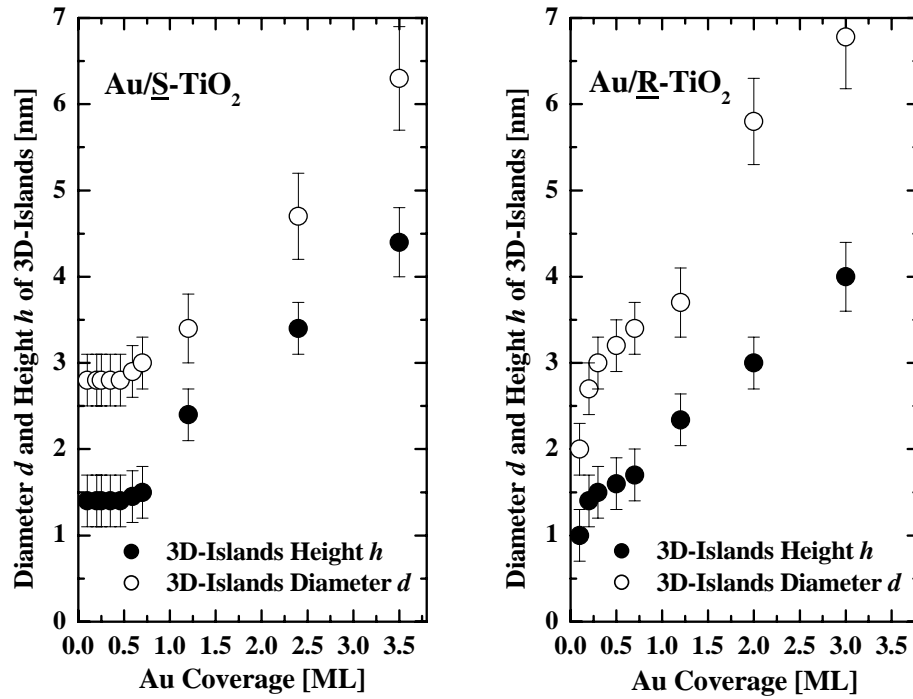


FIG.3. Average height h and diameter d of partial sphere giving the best-fit of MEIS spectra for stoichiometric (left) and reduced (right) TiO_2 substrates.

Au(111) surface[30]. Careful reading the Fermi edges indicates that the Au nano-clusters become metallic for Au coverage above 0.7 ML (diameter: 3 - 3.5 nm). Another information obtained from the valence band spectra is the fact that the two peaks originating from the O 2p bonding and nonbonding states shift slightly toward lower binding energy by 0.2 ± 0.05 eV by Au deposition. As will be discussed later, this is ascribed to relaxation of downward band bending to some extent by Au deposition.

Figure 6 shows the Ti 3p spectra (left side) and valence band spectra (right side) observed for the reduced $\text{TiO}_2(110)$ surface and that exposed to O_2 for 100 s at a pressure of 1×10^{-5} Torr. The samples were prepared by annealing at 550°C for 5 min in UHV (bottom), then exposed to O_2 (exposure of 1000 L: middle) at RT and annealed again at 550°C for 5 min in UHV (top). As mentioned earlier, removal of a neutral oxygen atom (bridging O on top) leaves behind two electrons (3d from the underlying Ti ion) which previously occupied O 2p

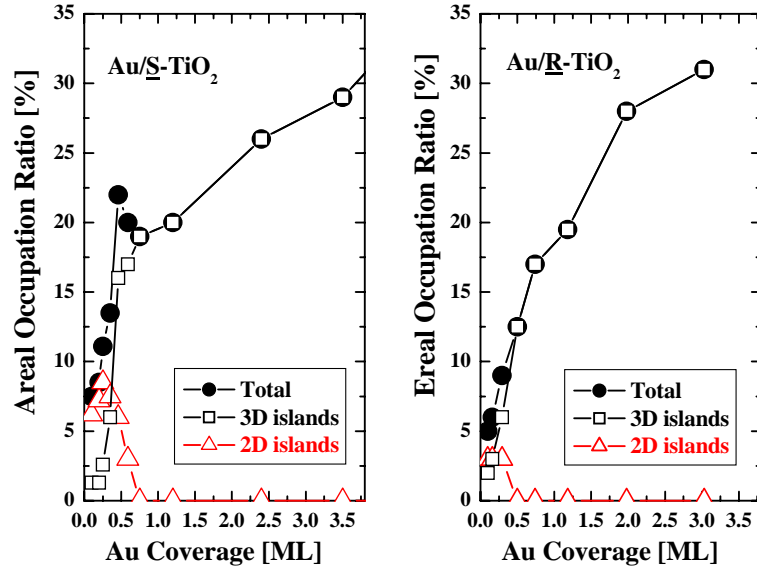


FIG.4. Areal occupation ratios of 2D (triangles) and 3D (squares) islands together with total (full circles) occupation ratios (2D + 3D) as a function of Au coverage supported on stoichiometric (left) and reduced (right) TiO₂ substrates.

state in the valence band. The extra electrons in the vacancies act as donor-like surface states that create an accumulation layer (probably very thin, less than 1 nm) in the near surface region[25,26]. Such an electron charge transfer generates a surface dipole with a positively charged top surface and negatively charged accumulation layer in the substrate (n-type). Thus downward band-bending occurs (see Fig. 7). Indeed, the Ti 3p and O 2p bonding and nonbonding peaks for the reduced surface shift to higher binding energy by 0.2-0.25±0.05 eV compared with those for the stoichiometric surface. In order to interpret the observed higher binding energy shifts of the Ti 3p and higher peak energy shifts of the O-2p band, it is essential to consider downward band bending rather than chemical shifts. Here, it must be noted that the number of O-vacancies on top is about 8 % of the surface bridging oxygen. However, the dipole field covers a surface region in a semi-macroscopic scale.

The binding energy of Ti 3p scaled from the Fermi level is indicated as a function of Au

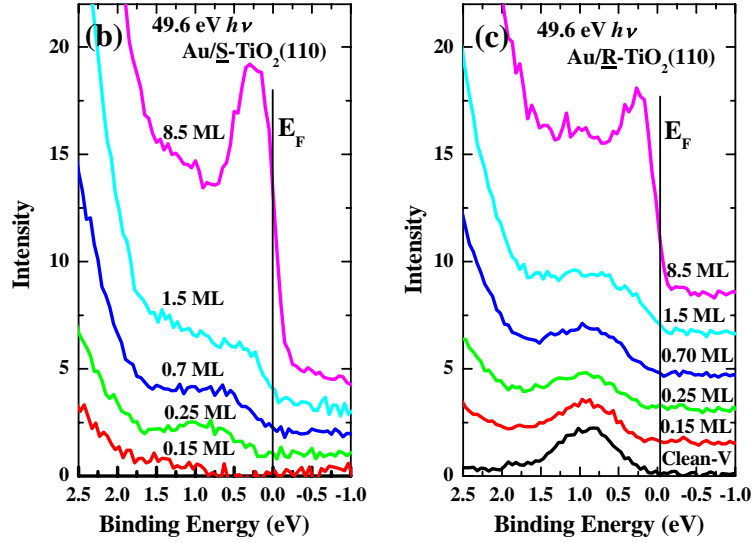


FIG.5. (a) Valence band spectra observed at photon energy of 49.6 eV for reduced $\text{TiO}_2(110)$ support before and after Au deposition under normal emission condition. Magnified valence band spectra near the Fermi level for (b) stoichiometric and (c) reduced TiO_2 substrates.

coverage for the S- and R- $\text{TiO}_2(110)$ substrates (see Fig.8). A small amount of Au deposition (0.15 ML) on the R- TiO_2 surface decreases the E_B value by 0.15 eV and the E_B value is almost constant by additional Au deposition. This indicates that the electron-deficiency at the O-vacancy sites is partly filled by electron charge transfer from Au. In fact, as shown later, we observed higher binding energy shifts of Au 4f even at a small Au coverage for both substrates indicating an electron charge transfer from Au to TiO_2 substrates (see Fig. 7). In the case of the S- TiO_2 substrate, slightly downward band-bending takes place due to an electron charge transfer from Au to the TiO_2 substrate resulting in dipole formation at the Au/ TiO_2 interface. It is interesting that formation of Au nano-clusters on the S- and R- $\text{TiO}_2(110)$ substrates leads to a slight and almost the same band-bending downward.

Figure 9 shows the binding energy (E_B) of the Au $4f_{7/2}$ peak as a function of Au coverage for stoichiometric and reduced $\text{TiO}_2(110)$ and $\text{NiO}(001)$ substrates. Significant higher E_B shifts are seen for $\text{TiO}_2(110)$ substrates but no E_B shift for $\text{NiO}(001)$. The present result on

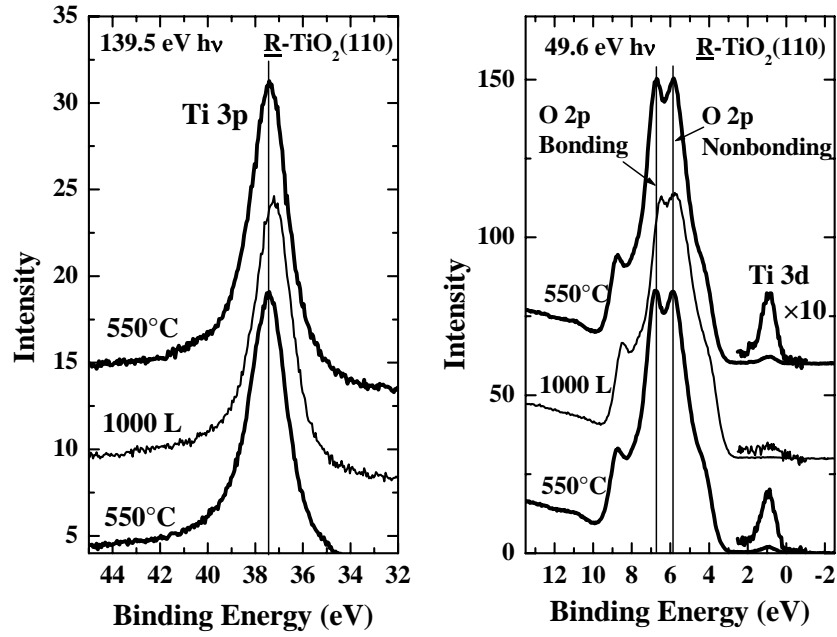


FIG. 6. Ti 3p (left) and valence band (right) spectra observed at photon energy of 139.5 and 49.6 eV, respectively under normal emission condition for reduced $\text{TiO}_2(110)$ surface and that exposed to O_2 for 100 s at a pressure of 1×10^{-5} Torr (corresponding to an exposure of 1000 L, 1 L = 10^{-6} Torr s). The samples were prepared by annealing at 550°C for 5 min in UHV (bottom), then exposed to O_2 (1000 L: middle) at RT and annealed again at 550 °C for 5 min in UHV (top). The peak (valence band) centered about 1 eV below the Fermi level comes from 3d electrons of Ti neighboring an O-vacancy.

the Au $4f_{7/2}$ E_B shift is consistent with the result reported by Howard et al.[16] and Sykes et al.[31]. Based on the density functional calculations, Wahlström et al.[17] reported no significant charge transfer between Au and TiO_2 . On the other hand, Vijay and Mills[21] predicted a substantial electron charge transfer from TiO_2 to Au. Minato et al.[9] observed lower binding energy shifts of O 2p nonbonding state and decrease in Ti 3d peak area with increasing Au coverage on significantly reduced $\text{TiO}_2(110)$ substrates and regarded the results as electron charge transfer from the surface defects to Au clusters. However, the observed higher E_B shifts unambiguously indicate an electron charge transfer from Au to TiO_2 substrates. As mentioned before, the lower binding energy shifts of O 2p nonbonding state

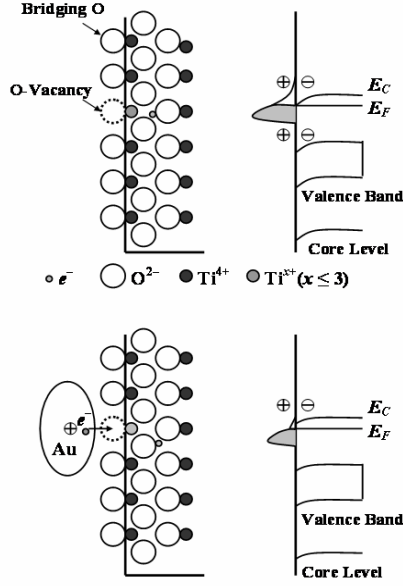


FIG. 7. Schematics of near surface regions of R-TiO₂(110) and Au/R-TiO₂(110) (left) together with band bending due to donor-like surface states and relaxation of band bending due to electron charge transfer from Au to O-vacancy site (right).

and the decrease in Ti 3d are explained by electron supply to O-vacancy sites (electron deficient) and the resultant relaxation of the downward band bending. The electron charge transfer from Au to O-vacancy sites reduces the density of states of the surface state band. The smaller E_B shifts for the reduced TiO₂ surface compared with the stoichiometric surface are due to the fact that the surface dipole of the R-TiO₂(110) resulting in downward band bending has a positive charge on top (electron-deficient) and a negatively charged accumulation layer inside. Therefore, the electrons from Au cancel the positive charge on top partly but the diffusion inside is significantly suppressed by the negatively charged accumulation layer. As a result, the electron charge transfer from Au to R-TiO₂(110) is diminished rather than that to S-TiO₂(110) substrate. With increasing Au coverage, the E_B value decreases and reaches that of bulk Au at Au coverage of 8 ML. The electron charge transfer from Au to TiO₂ substrates induces an interface dipole, whose electric field is screened more strongly with increasing the size of Au nano-particles. Here, we must note that the escape depth of the photoelectrons with kinetic energy of 50-60 eV is very short about 4 Å[32].

Finally, we determined the work functions (Φ) for both Au/S-TiO₂(110) and Au/R-TiO₂(110) surfaces. The sample was negatively biased ($V = -7.6$ V) and the energy

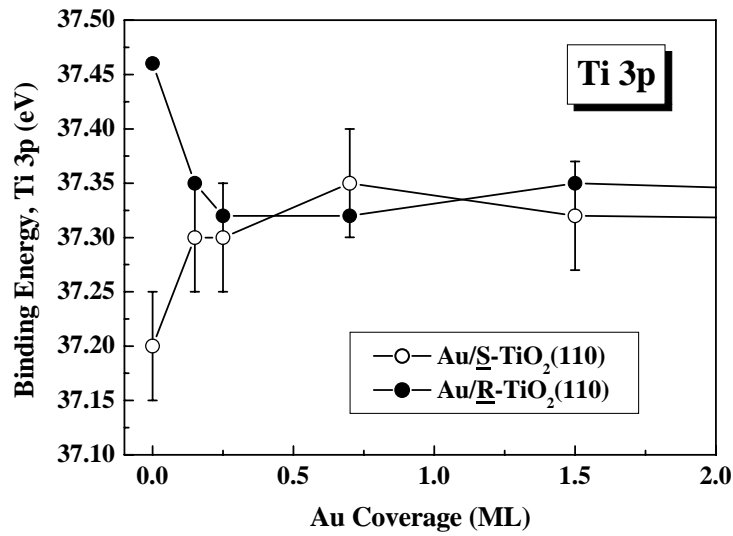


FIG.8. Observed binding energy of Ti 3p peaks as a function of Au coverage for stoichiometric (open circles) and reduced (full circles) TiO₂(110) supports. The uncertainties for Au/R-TiO₂ are almost the same as those for Au/S-TiO₂.

spectrum of the emitted photoelectrons was observed[19,33]. Figure 10 shows the work functions as a function of Au coverage. The work function of the R-TiO₂ surface is significantly smaller than that of the S-TiO₂ surface. This is ascribed to the fact that the R-TiO₂ surface has a dipole with a positive charge on the vacuum side resulting in a downward band bending, which reduces the work function. Remarkable drops of the work function by Au deposition of 0.1 – 1.5 ML on the S-TiO₂ surface is correlated with an electron charge transfer taking place from Au to TiO₂ substrate, which is evidenced from the higher binding energy shifts of Au 4f for Au coverage of 0.15 and 1.5 ML. Here, we must note that an electric field generated on the vacuum side acts on emitted electrons and the work done against the field from the top surface to a region far from the surface corresponds to the work function. As a probable mechanism, the interface dipole induced by electron charge transfer from Au to TiO₂ reduces the work function. The electric field generated by the interface dipole is screened completely by thick Au over-layers for Au coverage above 8 ML (the areal occupation ratio of Au is more than 80 %). In the case of Au deposition on the

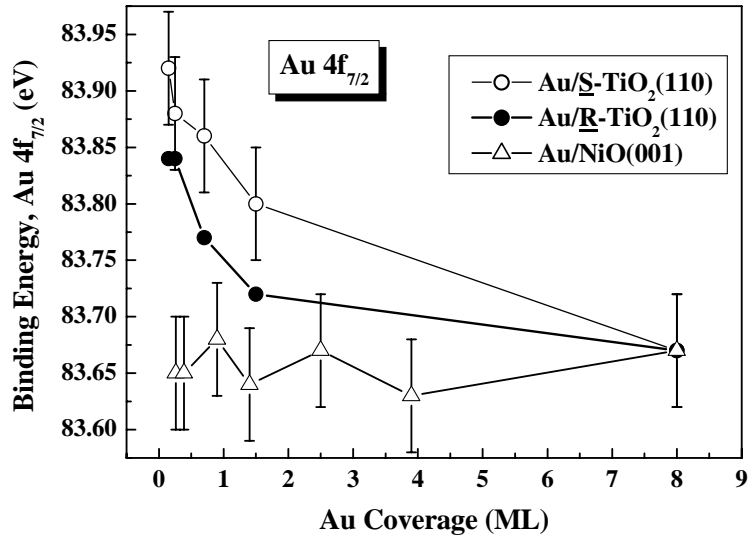


FIG.9. Observed binding energy of Au $4f_{7/2}$ peaks as a function of Au coverage for NiO(001) (open triangles), reduced (full circles) and stoichiometric (open circles) $\text{TiO}_2(110)$ substrates. The Au $4f_{5/2,7/2}$ core level spectra were observed at photon energy of 139.5 eV under normal emission condition (not shown here).

R- $\text{TiO}_2(110)$ substrate, the surface dipole giving the downward band bending is relaxed by Au nucleation at the O-vacancy site. Electron charge transfer from Au to R- TiO_2 substrate is smaller than that for S- TiO_2 because electron diffusion into the R-substrate is significantly suppressed by the accumulation layer. In fact, the Au $4f_{7/2}$ binding energy shifts for R- TiO_2 is smaller than those for S- TiO_2 . Coincidence within experimental uncertainty between the work functions of Au/S- TiO_2 and Au/R- TiO_2 for Au coverage above 0.15 ML is correlated with the binding energy shifts of Ti 3p (see Fig. 8).

4. Summary

The growth mode and electronic properties of Au nano-particles deposited on stoichiometric and reduced $\text{TiO}_2(110)$ surfaces were analyzed by high-resolution MEIS and SR-PES. In the case of S- $\text{TiO}_2(110)$, initially 2D-islands grow dominantly for Au coverage up to 0.5 ML and higher coverage increases the islands height to form 3D-islands for higher

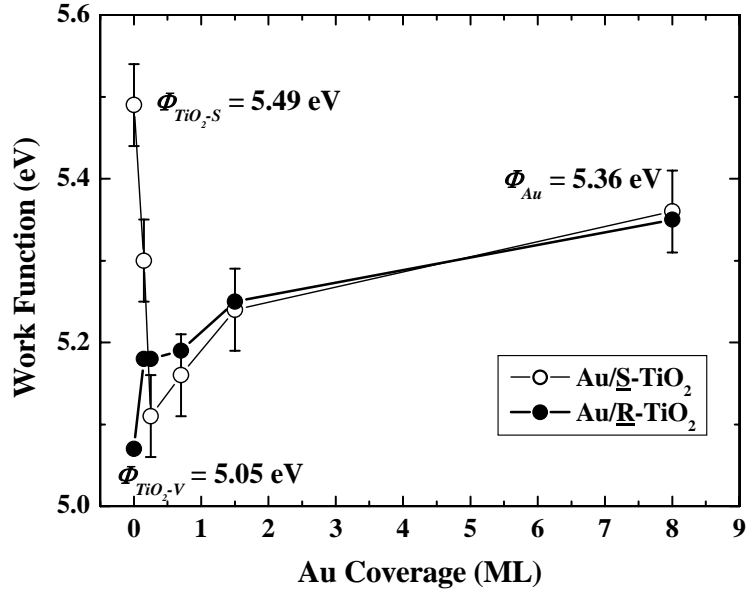


FIG. 10. Work functions determined by photoemission spectra for Au/S-TiO₂(110) (open circles) and Au/R-TiO₂(110) (full circles) as a function of Au coverage.

coverage. In contrast, 3D-islands start to grow at an early stage of Au deposition for the R-TiO₂(110). This is probably due to an O-vacancy acting as the nucleation site. The average 3D islands are well approximated by a partial sphere with a diameter d and height h , which range from 2.5 to 3.5 nm and from 1 to 2.5 nm, respectively for Au coverage from 0.1 up to 1.25 ML. The reduced TiO₂(110) surface prepared by annealing in UHV has bridging O vacancies of about 8 %, which was derived from high-resolution MEIS using ¹⁸O₂ adsorption. The observed valence band and Ti 3p spectra showed that the band is bent downward about 0.2 – 0.25 eV for R-TiO₂(110) in comparison with that for S-TiO₂(110) due to a donor-like surface state band induced by the surface O-vacancies. A small amount of Au deposition (0.15 ML) on the R-TiO₂ surface decreases the E_B value by 0.15 eV. This indicates that Au atoms nucleate at the O-vacancy sites and the positive charge (electron deficiency) of the top surface is partially canceled by an electron charge transfer from Au. In the case of the S-TiO₂ surface, a small Au deposition increases slightly the E_B value of Ti 3p due to downward band bending induced by an electron charge transfer from Au to TiO₂

substrates. Such electron charge transfer from Au to TiO₂ substrates is confirmed by higher binding energy shifts of Au 4f_{5/2,7/2} for both S- and R-TiO₂ surfaces. The work function of the R-TiO₂ surface is significantly smaller than that of the S-TiO₂ surface, due to the fact that the R-TiO₂ surface has a dipole with a positive charge on top of the surface, which reduces the work function. Remarkable drops of the work function by Au deposition of 0.15 – 1.5 ML on the S-TiO₂ surface is correlated with an electron charge transfer from Au to TiO₂ substrate. In the case of Au deposition on the R-TiO₂(110) substrate, the surface dipole giving the downward band bending is relaxed by Au nucleation at the O-vacancy site but the electron diffusion into the substrate is significantly suppressed due to the presence of the accumulation layer. Coincidence of the work function of Au/S-TiO₂ with that of Au/R-TiO₂ for Au coverage above 0.7 ML is correlated with the binding energy shifts of Ti 3p.

There are some theoretical predictions based on the density functional calculations concerning what is the decisive factor to enhance the catalytic activity of Au nano-particles supported on transition-metal oxides. According to Liu et al.[12], positively charged Ti at the Au/TiO₂ interface enhances electron charge transfer from Au to the 2π orbitals of adsorbed O₂, as a result O₂ is highly activated and CO oxidation occurs at the interface with a very low potential barrier. Molina et al.[13] reported that the presence of a supported Au particle strongly stabilizes the adsorption of O₂ and a sizable electronic charge transfer takes place from Au to the O₂ and the TiO₂ support. The O₂ can react with CO adsorbed at the interfacial perimeter of the Au particles leading to the formation of CO₂ with a very low energy barrier. The present work provides the electronic properties of Au nano-particles supported on S- and R-TiO₂(110). In the next study, the adsorption sites of O₂ and CO and the electronic structures of the adsorbed Au/TiO₂ will be manifested using isotopically labeled ¹⁸O₂ and ¹²C¹⁸O.

Acknowledgements

The authors would like to thank Dr. K. Okazaki and Dr. T. Akita for useful discussions

and comments. Special thanks are also due to Dr. T. Nishimura and Mr. M. Fujiwara for supporting the MEIS and PES experiments. Prof. H. Namba and Dr. K. Ogawa are also acknowledged for their maintaining the SORIS Beam-Line. This work was partly supported by the Fellowship of the Japan Society for the Promotion of Science (JSPS) for Young Scientists.

References

- [1] M. Haruta, T. Kobayashi, H. Sano and N. Yamada, *Chem. Lett.* **2** (1087) 405.
- [2] M. Haruta, N. Yamada, T. Kobayashi and S. Iijima, *J. Catal.* **115** (1989) 31.
- [3] B. Hammer and J.K. Nørskov, *Nature* **376** (1995) 238.
- [4] Y. Iizuka, H. Fujiki, N. Yamauchi, T. Chijiwa, S. Arai, S. Tsubota and M. Haruta, *Catal. Today* **36** (1997) 115.
- [5] M. Haruta, *Catal. Today* **36** (1997) 153.
- [6] C. Xu, W.S. Oh, G. Liu, D.Y. Kim and D.W. Goodman, *J. Vac. Sci. Technol.* **A 15** (1997) 1261.
- [7] S.C. Parker, A.W. Grant, V.A. Bondzie and C.T. Campbell, *Surf. Sci.* **441** (1999) 10.
- [8] F. Cosandey, L. Zhang and T.E. Madey, *Surf. Sci.* **474** (2001) 1.
- [9] T. Minato, T. Susaki, S. Shiraki, H.S. Kato, M. Kawai and K. Aika, *Surf. Sci.* **566-568** (2004) 1012.
- [10] S. Lee, C. Fan, T. Wu and S.L. Anderson, *Surf. Sci.* **578** (2005) 5.
- [11] N. Lopez and J.K. Nørskov, *Surf. Sci.* **515** (2002) 175.
- [12] Z.-P. Liu, X.-Q. Gong, J. Kohanoff, C. Sanchez and P. Hu, *Phys. Rev. Lett.* **91** (2003) 266102.
- [13] L.M. Molina, M.D. Rasmussen and B. Hammer, *J. Chem. Phys.* **120** (2004) 7673.
- [14] M. Valden, X. Lai and D.W. Goodman, *Science* **281** (1998) 1647.
- [15] C.E.J. Mitchell, A. Howard, M. Carney and R.G. Egdell, *Surf. Sci.* **490** (2001) 196.
- [16] A. Howard, D.N.S. Clark, C.E.J. Mitchell, R.G. Egdell and V.R. Dhanak, *Surf. Sci.* **518** (2002) 210.
- [17] E. Wahlström, N. Lopez, R. Schaub, P. Thorstrup, A. Rønnau, C. Africh, E. Lægsgaard, J.K. Nørskov and F. Besenbacher, *Phys. Rev. Lett.* **90** (2003) 026101.
- [18] Y. Maeda, M. Okumura, S. Tsubota, M. Kohyama and M. Haruta, *Appl. Surf. Sci.* **222** (2004) 409.

- [19] T. Okazawa, M. Fujiwara, T. Nishimura, T. Akita, M. Kohyama and Y. Kido, *Surf. Sci.* **600** (2006) 1331.
- [20] A. Vittadini and A. Selloni, *J. Chem. Phys.* **117** (2002) 353.
- [21] A. Vijay, G. Mills and H. Metiu, *J. Chem. Phys.* **118** (2003) 6536.
- [22] K. Okazaki, Y. Morikawa, S. Tanaka, K. Tanaka and M. Kohyama, *Phys. Rev.* **B 69** (2004) 235404.
- [23] J.F. van der Veen, *Surf. Sci. Rep.* **5** (1985) 199.
- [24] Y. Kido, T. Nishimura, Y. Hoshino and H. Namba, *Nucl. Instrum. Methods* **B161-163** (2000) 371.
- [25] U. Diebold, *Surf. Sci. Report* **48** (2003) 53.
- [26] Z. Zhang, S.-P. Jeng and V.E. Henrich, *Phys. Rev.* **B 43** (1991) 12004.
- [27] G. Charlton, P.B. Howes, C.L. Nicklin, P. Steadman, J.S.G. Taylor, C.A. Muryn, S.P. Harte, J. Mercer, R. McGrath, D. Norman, T.S. Turner and G. Thornton, *Phys. Rev. Lett.* **78** (1997) 495.
- [28] J.-M. Pan, B.L. Maschhoff, U. Diebold and T.E. Madey, *J. Vac. Sci. Technol.* **A 10** (1992) 2470.
- [29] Y. Kido and T. Koshikawa, *J. Appl. Phys.* **67** (1990) 187.
- [30] S. Hüfner, *Photoelectron Spectroscopy*, Springer-Verlag, New York, 1996.
- [31] E.C.H. Sykes, F.J. Williams, M.S. Tikhov and R.M. Lambert, *J. Phys. Chem.* **B 106** (2002) 5390.
- [32] S. Tanuma, T. Shiratori, T. Kimura, K. Goto, S. Ichimura and C.J. Powell, *Surf. Interface Anal.* **37** (2005) 833.
- [33] T. Nishimura, J. Takeda, Y. Asami, Y. Hoshino and Y. Kido, *Surf. Sci.* **588** (2005) 71.